Evaluation and Optimization of Nonlinear Central Pattern Generators for Robotic Locomotion

Abdalftah Elbori*, Mehmet Turan, Kutluk Bilge Arikan*****

** Department of Mathematics Azzaytuna University, Tarhuna-Libya*
e-mail: abdalftah81@yahoo.com
***Department of Mathematics Atılım University, 06836, Ankara-Turkey*
e-mail: mehmet.turan@atilim.edu.tr
****Department of Mechanical Engineering, TED University, 06420, Ankara-Turkey*
e-mail: kutluk.arikan@tedu.edu.tr

Abstract: With regard to the optimization of Central Pattern Generators (CPGs) for bipedal locomotion in robots, this paper investigates how the different cases of CPGs such as uncoupled, unidirectional, bidirectional two CPGs are used to produce rhythmic patterns for one leg with two degrees of freedom (DOF). This paper also discusses the stability analysis of CPGs and attempts to utilize genetic algorithms with the hybrid function and adapts the CPGs to robotic systems that perform one-leg movement, by utilizing the bidirectional two CPGs. The results show far greater improvement than in the other cases. CPGs not only enhance movement but also control locomotion without any sensory feedback.

Keywords: Central Patterns Generators (CPGs), one leg model, a strategy to couple CPGs, stability analysis, optimizing CPGs.

1. INTRODUCTION

Locomotion of robots is one of the most widely discussed topics with basic locomotors at the heart of investigations. In biological systems, a number of various patterns occur which are produced by a central nervous system such as, running, walking, swimming and crawling. The central nervous system is called Central Pattern Generator (CPG). The central nervous system of vertebrate and invertebrate animals locals in the spinal cord as shown by some researches (Ijspeert, 2008; Sillar, 1996). Some studies have shown that there are functions in the human body, for instance breathing and digestion, that cannot be controlled consciously, but controlled by CPGs (Ijspeert, 2008; Billard and Ijspeert, 2000).

Biologically, CPGs can be defined as inspired networks of nonlinear oscillating neurons capable of generating rhythmic patterns without higher control centres or sensory feedback. A neural oscillator comprises a pair of neurons with inhibitive connections between them. Each neuron suppresses the other, which are a flexor and an extensor neuron (Bucheret et al., 2000; Casasnovas and Meyrand, 1995; Van Vreeswijk et al., 1994). It should be known that a single CPG is not a small neural network. Rather, it receives inputs from the higher parts of control centres (Ijspeert, 2008; Sillar, 1996).

Various mathematical and physical structures of the legs and limbs have been modeled (Williamson, 1999; Arikan and Irfanoglu, 2011; Abdalftah Elbori et al., 2017) and the control systems have been copied to reproduce patterns of movement in robots similar to those in certain biological organisms. When the body initiates movement, CPGs commence synchronization and send signals to neurons simultaneously in a movement cycle (Kimura et al., 2007; Wu et al., 2013).

Interestingly, various mathematical structures in the literature have modelled and mimicked biological control parameters (Williamson, 1999; Amrollah and Henaff, 2010; Ijspeert and Cabelguen, 2006; Jiaqi et al., 2011). Various CPG models, including the connectionist models, have been implemented in the robotic systems (Arena, 2000; Lu et al., 2005). Also, there are some studies discussing how systems of oscillators can be coupled (Crespi and Ijspeert, 2006; Ijspeert and Crespi, 2007; Ijspeert et al., 2007; Kimura et al., 1999).

Recently, various CPGs models have been implemented and designed in order to control bipedal locomotion in humanoid robots (Jiaqi et al., 2011; Taga, 1998; Taga et al., 1991). Also, different kinds of robots and modes of locomotion have been controlled using CPGs. The locomotion of hexapod and octopod robots is employed in some different CPG models (Arena et al., 2004; Inagaki et al., 2006; Inagaki et al., 2003). Also, CPGs are used to control swimming robots, for instance swimming lamprey or eel robots (Ijspeert and Crespi, 2007; Inagaki et al., 2006; Arena, 2001; Crespi and Ijspeert, 2008), as well as to control quadruped robots (Billard and Ijspeert, 2000; Brambilla et al., 2006; Fukuoka et al., 2003). For some studies that explored how one can use CPGs to control bipedal locomotion, we refer the reader to (Ishiguro et al., 2003; Pinto and Golubitsky, 2006; Wang et al., 2014; Arikan and Irfanoglu, 2011; Inada and Ishii, 2003; Abdalftah Elbori et al., 2017; Aoi and Tsuchiya, 2005; Endo et al., 2005; Torres-Huitzil and Girau, 2008; Nachstedt et al., 2017). Some of these studies have been considered the Van der Pol and the Hopf oscillator. Others used different mathematical structures of CPGs to control bipedal locomotion.

This paper mainly focuses on the analysis and optimization of the central pattern generators in details for the purpose of locomotion. If we want to apply the optimized patterns for the bipedal locomotion, the dynamical stability of the robot must be ensured by using the ZMP (zero moment point) technique. In this case, the patterns may be modulated to guarantee the stability which is shaped by the ZMP analysis. In addition, the torso may be activated to improve the dynamical stability of the bipedal robot. This paper draws on and derives support from the studies mentioned above and investigates how CPGs can be optimized for bipedal locomotion via an adaptation to the robotic systems that perform one leg movement. In particular, this paper investigates a nonlinear limit-cycle oscillator similar to the Van der Pol oscillator. It combines both oscillators to control the swing phase of the kinematic model of a single leg system. The mathematical analysis for the optimization of the CPG can be another novelty in this paper. Based on the cost function, this paper uses a developmental algorithm to find the optimum parametric values for two CPGs in three different cases, it is predicted that the bidirectional two CPGs will give the best results.

The paper is organized as follows: The kinematic model has been discussed in the next section. A strategy to couple two CPGs is given in Section 3. In Section 4, the stability analysis is discussed. Section 5 is devoted to the optimization results. In Section 6, some conclusions are drawn and suggestions for future research are given.

2. KINEMATIC MODEL

Economically speaking, the kinematic model is designed to conduct a base analysis. Fig 1 presents the leg structure in two cases of motion: a swing mode and a stance mode. There, L_1 and L_2 are the lengths from the hip joint to the knee joint, and from the knee joint to the end effector, respectively; and θ_1 is the angular position of the hip and θ_2 is the angular position of the knee, y_g is the distance between the lower body and the ground. The coordinates of the lowest part of the hip and knee are denoted by (x_A, y_A) and (x_f, y_f), respectively.

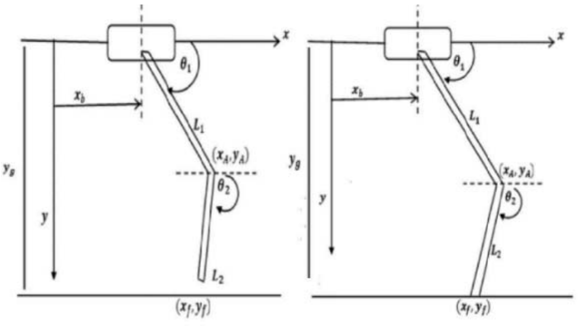

Fig. 1. Swing and stance modes of the leg.

There are two cases to consider during motion. The first case is when $y_f = y_g$, that is, the leg touches the ground. This case is known as the stance mode in which case the leg behaves as a revolute joint. In stance mode, the hip joint angle θ_1 is computed in terms of the knee angle θ_2, which is established by the CPGs. Thus, in this mode, the kinematic model has one degree of freedom (DOF). Moreover, only in stance mode will the body move. The second case is when $y_f < y_g$, which is the time when the leg does not touch the ground. This mode is known as the swing mode. In this mode, the DOF is two, and the angles of both the hip and knee are calculated by two different CPGs.

The simple kinematic equations are

$$x_A = x_b + L_1 \cos\theta_1, \quad y_A = L_1 \sin\theta_1,$$

and

$$x_f = x_A + L_2 \cos\theta_2, \quad y_f = y_A + L_2 \sin\theta_2$$

which are considered in the sagittal plane. Additionally, the lower body is parallel to the ground during the locomotion, as in the Test Bench, where the hip joint height is fixed. Since the stability during the locomotion is guaranteed, the dynamic equations are not needed (See Fig 2 below.)

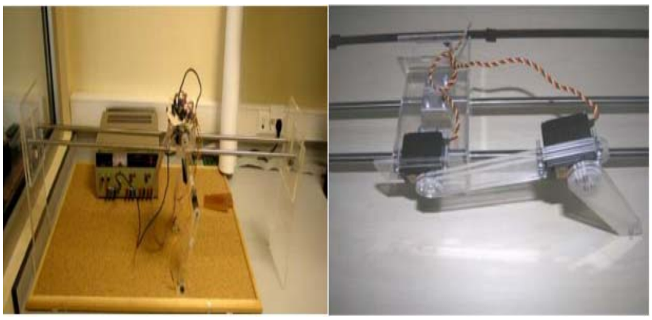

Fig. 2. The physical system and a closer view of the actuators of one leg of the Test Bench.

3. A STRAGETRY TO COUPLE THE CPGs

As stated previously, the CPG unit is responsible for generating the required angular signals for both joints. Such CPGs are furthered in mathematical equations and presented in general formulas (for details, see (Marbach, 2004; Van den Kieboom, 2009)). The sinusoidal signals are the appropriate function for locomotion control:

$$x = A\sin(2\pi f t + \varphi)$$

where A, f and φ are the amplitude, frequency and phase respectively. Differentiating x twice yields the system

$$\tau\,\dot{x} = v,\ \ \tau\,\dot{v} = -x,\ \ \tau = \frac{1}{2\pi f}$$

Here, the amplitude is implicitly defined by the system. In fact, it relies on the initial conditions. Therefore, to force the system to lead to a limit cycle with the desired amplitude, a new term should be included in the system. For example, the new system of differential equations may look like

$$\left.\begin{aligned} &\tau\,\dot{x} = v \\ &\tau\,\dot{v} = -\frac{\alpha}{E}\left(x^2 + v^2 - E\right)v - x \end{aligned}\right\} \qquad (1)$$

in which the parameters τ, α and E are positive constants. In (1), the term $x^2 + v^2$ stands for the actual energy and the difference $x^2 + v^2 - E$ denotes the error in the energy of the oscillator. Therefore, the newly added term may be considered the normalized energy.

To reach the strength of coupling CPGs, we consider a simple coupling strategy given in (Ijspeert and Cabelguen, 2006) is considered where each CPG sends a signal proportional to the states variables to every other CPG. More specifically, the system

$$\left.\begin{aligned} \tau\, \dot{x}_i &= v_i \\ \tau\, \dot{v}_i &= -\frac{\alpha}{E_i}\left(x_i^2+v_i^2-E_i\right)v_i - x_i + \sum_j \frac{a_{ij}x_j+b_{ij}v_j}{\sqrt{x_j^2+v_j^2}} \end{aligned}\right\} \tag{2}$$

will be considered. In (2), a_{ij} and b_{ij} are positive constants that determine how oscillator j influences oscillator i. Specific forms of outputs can still occur by means of changing the numerical values of the parameters (Amrollah and Henaff, 2010). Depending on the values of a_{ij} and b_{ij} the coupling weights of CPGs may be called uncoupled, unidirectional and bidirectional. The corresponding systems of differential equations are provided below:

$$\left.\begin{aligned} \tau\, \dot{x}_1 &= v_1 \\ \tau\, \dot{v}_1 &= -\frac{\alpha_1}{E_1}\left(x_1^2+v_1^2-E_1\right)v_1 - x_1 \\ \tau\, \dot{x}_2 &= v_2 \\ \tau\, \dot{v}_2 &= -\frac{\alpha_2}{E_2}\left(x_2^2+v_2^2-E_2\right)v_2 - x_2 \end{aligned}\right\} \tag{3}$$

$$\left.\begin{aligned} \tau\, \dot{x}_1 &= v_1 \\ \tau\, \dot{v}_1 &= -\frac{\alpha_1}{E_1}\left(x_1^2+v_1^2-E_1\right)v_1 - x_1 + \frac{a_{12}x_2+b_{12}v_2}{\sqrt{x_2^2+v_2^2}} \\ \tau\, \dot{x}_2 &= v_2 \\ \tau\, \dot{v}_2 &= -\frac{\alpha_2}{E_2}\left(x_2^2+v_2^2-E_2\right)v_2 - x_2 \end{aligned}\right\} \tag{4}$$

and

$$\left.\begin{aligned} \tau\, \dot{x}_1 &= v_1 \\ \tau\, \dot{v}_1 &= -\frac{\alpha_1}{E_1}\left(x_1^2+v_1^2-E_1\right)v_1 - x_1 + \frac{a_{12}x_2+b_{12}v_2}{\sqrt{x_2^2+v_2^2}} \\ \tau\, \dot{x}_2 &= v_2 \\ \tau\, \dot{v}_2 &= -\frac{\alpha_2}{E_2}\left(x_2^2+v_2^2-E_2\right)v_2 - x_2 + \frac{a_{21}x_1+b_{21}v_1}{\sqrt{x_1^2+v_1^2}} \end{aligned}\right\} \tag{5}$$

System (3) is called uncoupled because the two CPGs occurring in the system work independently. On the other hand, in system (4), there is a signal transfer from the second CPG to the first one, and that transfer is one way. This is why it is called unidirectional. Finally, in system (5), each CPG gives reference to the other CPG. Therefore, it is called bidirectional coupling. In any case, the outputs are $x_1 = \theta_1$ and $x_2 = \theta_2$, where θ_1 and θ_2, as defined in the kinematic model, represent the angular positions of the hip and knee, respectively.

4. STABILITY ANALYSIS

In this part, the stability analysis for each type of coupling given in the previous section will be discussed. For each case, a figure will be provided to illustrate the existence of a limit cycle.

4.1 Uncouple Two CPGs

As stated previously, uncoupled two CPGs consist of four differential equations given in (3). These four differential equations represent two independent CPGs. Therefore, it is sufficient to analyze one of them to understand the stability of the system. For (1), which is a nonlinear system, clearly the origin is the only fixed point and the linearized system at the fixed point has the Jacobian matrix

$$J(0,0) = \begin{bmatrix} 0 & 1/\tau \\ -1/\tau & \alpha/\tau \end{bmatrix}$$

whose eigenvalues are $\lambda_{1,2} = \left(\alpha \pm \sqrt{\alpha^2-4}\right)/(2\tau)$. Since $\alpha/\tau > 0$, the fixed point is locally unstable. Let's consider (1) in polar coordinates: $x = r\cos\theta$, $v = r\sin\theta$. Then, (1) becomes

$$\begin{aligned} \dot{r} &= \frac{\alpha}{\tau E} r\left(E-r^2\right)\sin^2\theta \\ \dot{\theta} &= \frac{1}{\tau} - \frac{\alpha}{\tau E}\left(r^2-E\right)\sin\theta\cos\theta \end{aligned}$$

It is now obvious that all solutions with $r(0) > 0$ tend to $\sqrt{E}$ as $t \longrightarrow \infty$. Translating this into the x, y plane, it means that x^2+v^2 increases as long as $x^2+v^2 < E$, and it decreases when $x^2+v^2 > E$. Thus, there is a stable limit cycle with radius $\sqrt{E}$ and an unstable equilibrium point at the origin. In Fig 3, two solutions corresponding to different values of the parameters for the first CPG are shown. The limit cycle for one CPG can be observed in that figure.

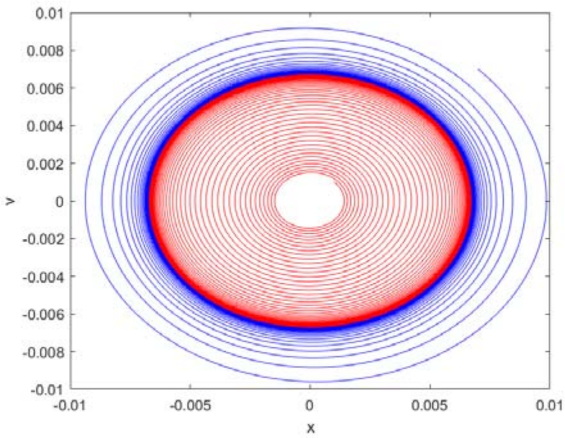

Fig. 3. Stable limit cycle of uncoupled single CPGs: Red curve correspond to the initial condition $\left(x_1(0), v_1(0)\right)$=(0.001, 0.001), and the blue solution corresponds to the initial condition $\left(x_1(0), v_1(0)\right)$=(0.007, 0.007). These different solutions correspond to the values τ=0.009, α=0.03 and E_1=0.000045.

4.2 Unidirectional Two CPGs

Unidirectional two CPGs consist of four differential equations given in (4). These four differential equations represent two dependent CPGs. It is clear that there is no equilibrium point for unidirectional two CPGs. To check whether there is a periodic solution, the change of variables

$$x_1 = r_1 \cos\theta_1, \quad v_1 = r_1 \sin\theta_1,$$
$$x_2 = r_2 \cos\theta_2, \quad v_2 = r_2 \sin\theta_2$$

are used. Then, in the new coordinate system, (4) becomes

$$\dot{r}_1 = -\frac{\alpha}{\tau E_1}\left(r_1^2 - E_1\right) r_1 \sin^2\theta_1 + \frac{1}{\tau}\left(a_{12}\cos\theta_2 + b_{12}\sin\theta_2\right)\sin\theta_1$$

$$\dot{\theta}_1 = -\frac{1}{\tau} - \frac{\alpha}{\tau E_1}\left(r_1^2 - E_1\right)\cos\theta_1 \sin\theta_1 + \frac{1}{\tau\, r_1^2}\left(a_{12}\cos\theta_2 + b_{12}\sin\theta_2\right)$$

$$\dot{r}_2 = -\frac{\alpha}{\tau E_2}\left(r_2^2 - E_2\right) r_2 \sin^2\theta_2$$

$$\dot{\theta}_2 = -\frac{1}{\tau} - \frac{\alpha}{\tau E_2}\left(r_2^2 - E_2\right)\cos\theta_2 \sin\theta_2$$

Clearly, $r_2 = \sqrt{E_2}$ is the periodic solution for the second CPG. The limit cycle for the first CPG can be observed in Fig 4. Therefore, as in the case of uncoupled two CPGs, this system has a limit cycle.

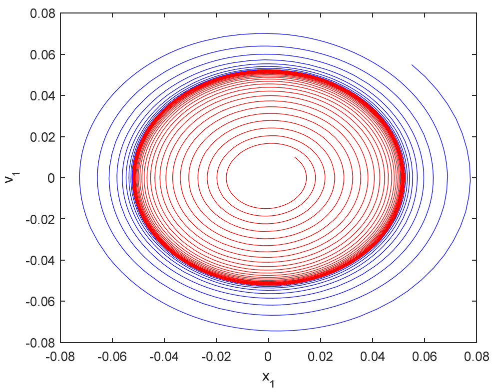

Fig. 4. Two trajectories of the first CPG in the case of unidirectional two CPGs: Red curve correspond to the initial condition $\left(x_1(0), v_1(0), x_2(0), v_2(0)\right) = (0.01, 0.01, 0.01, 0.01)$, and the blue solution corresponds to the initial condition $\left(x_1(0), v_1(0), x_2(0), v_2(0)\right) = (0.05, 0.05, 0.05, 0.05)$. These different solutions correspond to the values $\tau = 0.01$, $\alpha_1 = 0.0001$, $\alpha_2 = 0.001$, $a_{12} = b_{12} = 0.001$ and $E_1 = E_2 = 0.00001$

4.3 Bidirectional Two CPGs

The four differential equations in (5) represent two dependent CPGs. Note that for an equilibrium point the first and the third equations give $v_1 = v_2 = 0$ which leads to $-x_1 \pm a_{12} = 0$ and $-x_2 \pm a_{21} = 0$. It is clear that x_1 and x_2 should have the same signs, and the equilibrium points are $(a_{12}, 0, a_{21}, 0)$ and $(-a_{12}, 0, -a_{21}, 0)$. It should be mentioned here that, the points $(a_{12}, 0, -a_{21}, 0)$ and $(-a_{12}, 0, a_{21}, 0)$ are not equilibrium points. The Jacobian matrices at the fixed point are

$$J(\pm a_{12}, 0, \pm a_{21}, 0) = \begin{bmatrix} 0 & 1/\tau & 0 & 0 \\ -1/\tau & \alpha\left(E_1 - a_{12}^2\right)/(\tau E_1) & 0 & \pm b_{12}/(\tau a_{21}) \\ 0 & 0 & 0 & 1/\tau \\ 0 & \pm b_{21}/(\tau a_{12}) & -1/\tau & \alpha\left(E_2 - a_{21}^2\right)/(\tau E_2) \end{bmatrix}$$

Therefore, the eigenvalues for both equilibrium points are the roots of the characteristic equation

$$\left(\lambda^2 + \lambda\beta_1 + \frac{1}{\tau^2}\right)\left(\lambda^2 + \lambda\beta_2 + \frac{1}{\tau^2}\right) - \frac{\lambda^2}{\tau^2}\mu = 0 \qquad (6)$$

in which $\beta_1 = \frac{\alpha}{\tau E_1}(a_{12}^2 - E_1)$, $\beta_2 = \frac{\alpha}{\tau E_2}(a_{21}^2 - E_2)$, and $\mu = \frac{b_{12}b_{21}}{a_{12}a_{21}}$. The characteristic roots are

$$\lambda_{1,2} = \frac{1}{\tau}\left[\frac{1}{4}\left(-\tau\beta_1 - \tau\beta_2 + D\right) \pm \frac{\sqrt{2}}{4}\sqrt{\tau^2\left(\beta_1^2 + \beta_2^2\right) - \tau D\left(\beta_1 + \beta_2\right) + 2\mu - 8}\right]$$

and

$$\lambda_{3,4} = \frac{1}{\tau}\left[\frac{1}{4}\left(-\tau\beta_1 - \tau\beta_2 - D\right) \pm \frac{\sqrt{2}}{4}\sqrt{\tau^2\left(\beta_1^2 + \beta_2^2\right) + \tau D\left(\beta_1 + \beta_2\right) + 2\mu - 8}\right]$$

where

$$D = \sqrt{\tau^2\left(\beta_2^2 + \beta_1^2\right) - \tau\beta_1\beta_2 + 4\mu}$$

It is difficult to make the analysis in this. Thus, either one as to trust the simulation results only, which is not scientifically strong because of the errors that may occur during the computation, or one can consider special cases as we do here.

Case 1: *$\beta_1 = \beta_2 = \beta$. In that case, the eigenvalues are*

$$\lambda_{1,2} = \frac{-\beta\tau + \sqrt{\mu} \pm \sqrt{\beta^2\tau^2 - 2\beta\tau\sqrt{\mu} + \mu - 4}}{2\tau}$$

and

$$\lambda_{3,4} = \frac{-\beta\tau - \sqrt{\mu} \pm \sqrt{\beta^2\tau^2 + 2\beta\tau\sqrt{\mu} + \mu - 4}}{2\tau}$$

- When $\mu < 0$;
  - If *$\beta<0$*, then there are complex eigenvalues with positive real part. Hence, the fixed points an unstable source.
  - If *$\beta=0$*, then the eigenvalues are purely imaginary, and the system will oscillate around the steady state. The fixed points are stable.
  - If *$\beta>0$*, the real parts of all eigenvalues are negative. So, the fixed points are asymptotically stable.

These results are supported by Fig 5.

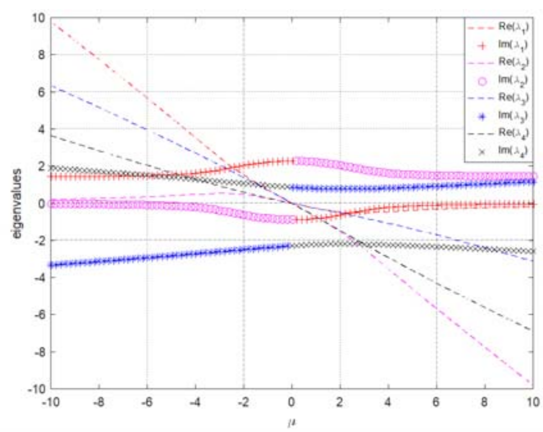

Fig. 5. The eigenvalues against β, when $\mu < 0$.

- When $\mu = 0$, as Fig 6 supports;
  - If $\beta<0$, then the eigenvalues are repeated and their real parts are positive. So, the fixed points are unstable.
  - If $\beta=0$, then the eigenvalues are repeated purely imaginary complex numbers. Thus, the fixed points are unstable.
  - If $\beta>0$, then the real parts of eigenvalues are negative. For $\tau_1 \neq \tau_2$ the fixed points are asymptotically stable and for $\tau_1 = \tau_2$ the eigenvalues are repeated which means that the fixed points are unstable.

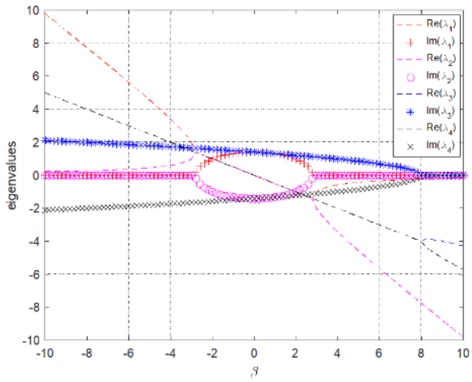

Fig. 6. The eigenvalues against β, when $\mu = 0$.

- When $\mu > 0$ as Fig 7 supports;
  - If $\beta<0$, then the eigenvalues have positive real parts. So, the fixed points are an unstable.
  - If $\beta>0$, the fixed points are stable for small values of μ and unstable for large values of μ.

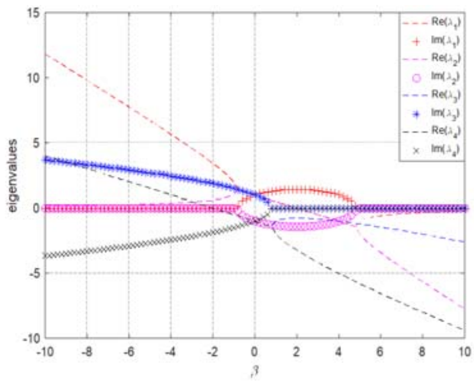

Fig. 7. The eigenvalues against β, when $\mu > 0$.

Case 2: $\beta_1 \neq \beta_2$.

- When $\mu < 0$, with the help of the Figs 8, 9, 10 and 11, one has;
  - If $\beta_1>0$, $\beta_2>0$, then the fixed points are stable.
  - If $\beta_1<0$, $\beta_2>0$, then the fixed points are stable for μ close to zero, otherwise the fixed points are unstable.
  - If $\beta_1>0$, $\beta_2<0$, then the fixed points are unstable.
  - If $\beta_1<0$, $\beta_2<0$, then the fixed points are unstable.
  - If $\beta_1=0$, then the fixed points are asymptotically stable for $\beta_2>0$ and they are unstable for $\beta_2<0$.
  - If $\beta_2=0$, then the fixed points are asymptotically stable for $\beta_1>0$ and they are unstable for $\beta_1<0$.

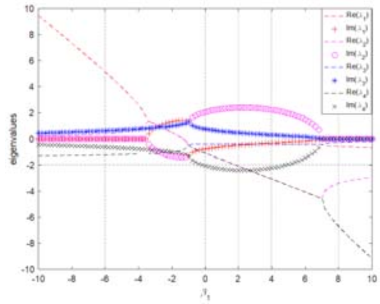

Fig. 8. The eigenvalues against β_1, when $\mu < 0$ and $\beta_2 > 0$.

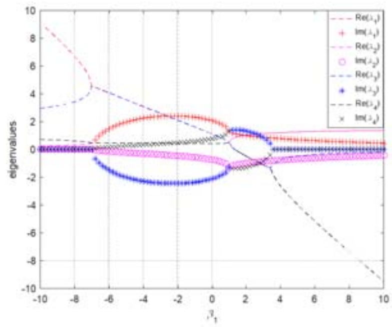

Fig. 9. The eigenvalues against β_1, when $\mu < 0$ and $\beta_2 < 0$.

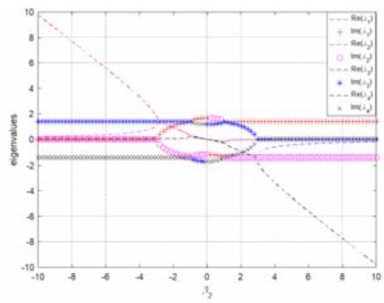

Fig. 10. The eigenvalues against β_2, when $\mu < 0$ and $\beta_1 = 0$.

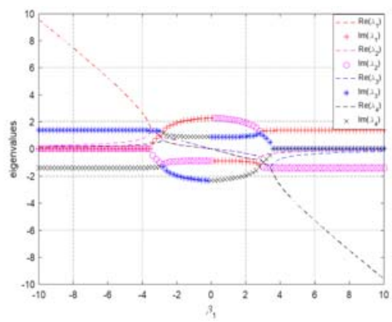

Fig. 11. The eigenvalues against β_1, when $\mu < 0$ and $\beta_2 = 0$

- When $\mu = 0$, with the help of the Figs 12, 13, 14 and 15, one has;
  - If $\beta_1>0$, $\beta_2>0$, then the fixed points are asymptotically stable.
  - If $\beta_1<0$, $\beta_2>0$, then the fixed points are unstable.
  - If $\beta_1>0$, $\beta_2<0$, then the fixed points are stable.
  - If $\beta_1<0$, $\beta_2<0$, then the fixed points are unstable.

- If $\beta_1=0$, then the fixed points are asymptotically stable for $\beta_2>0$ and they are unstable for $\beta_2<0$
- If $\beta_2=0$, then the fixed points are asymptotically stable for $\beta_1>0$ and they are unstable for $\beta_1<0$.

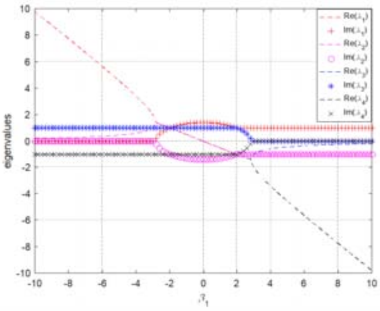

Fig. 12. The eigenvalues against β_1, when $\mu = 0$ and $\beta_2 > 0$.

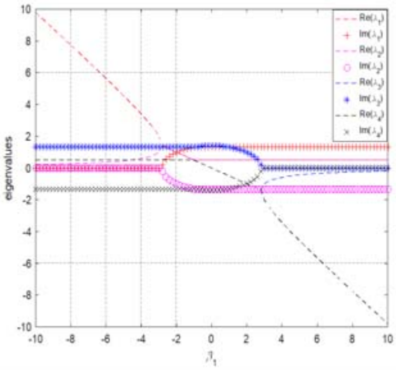

Fig. 13. The eigenvalues against β_1, when $\mu = 0$ and $\beta_2 < 0$.

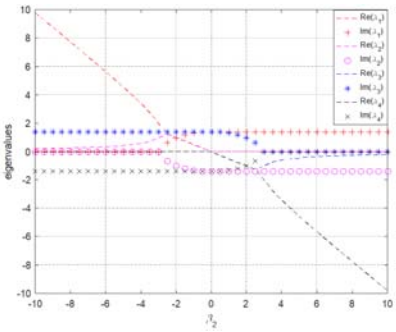

Fig. 14. The eigenvalues against β_2, when $\mu = 0$ and $\beta_1 = 0$.

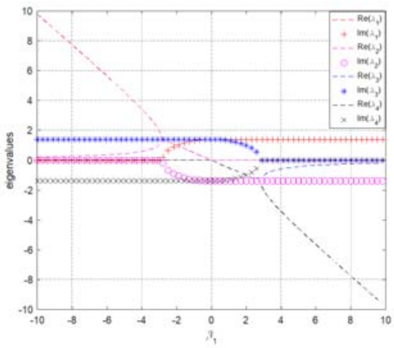

Fig. 15. The eigenvalues against β_1, when $\mu = 0$ and $\beta_2 = 0$.

- When $\mu > 0$, with the help of the Figs 16, 17, 18 and 19, one has;

- If $\beta_1>0$, $\beta_2>0$, then the fixed points are stable for μ close to zero, otherwise the fixed points are unstable.
- If $\beta_1<0$, $\beta_2>0$, then the fixed points are unstable.
- If $\beta_1>0$, $\beta_2<0$, then the fixed points are unstable.
- If $\beta_1<0$, $\beta_2<0$, then the fixed points are unstable.
- If $\beta_1=0$, then the fixed points are stable for $\beta_2>0$, or $\beta_2<0$ when μ close to zero, otherwise the fixed points are unstable.
- If $\beta_2=0$, then the fixed points are unstable for $\beta_1<0$, and $\beta_1>0$.

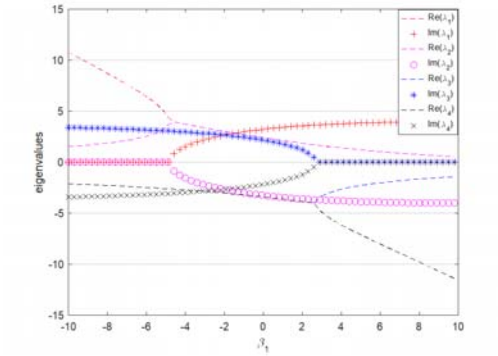

Fig. 16. The eigenvalues against β_1, when $\mu > 0$ and $\beta_2 > 0$.

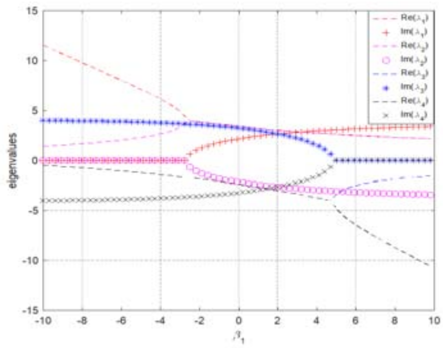

Fig. 17. The eigenvalues against β_1, when $\mu > 0$ and $\beta_2 < 0$.

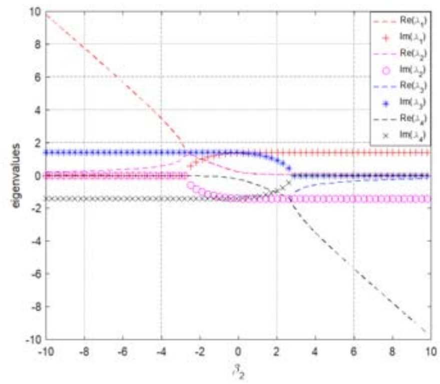

Fig. 18. The eigenvalues against β_2, when $\mu > 0$ and $\beta_1 = 0$.

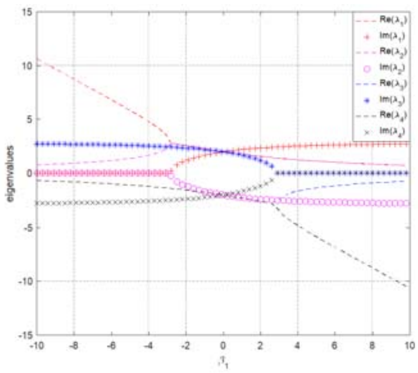

Fig. 19. The eigenvalues against β_1, when $\mu > 0$ and $\beta_2 = 0$.

5. OPTIMIZATION RESULTS

It is important to mention here that each CPG produces angular patterns as outputs for each joint. To estimate gait generation, it is essential to compute the optimal parameter sets for each CPG. In other words, it is necessary to understand how the angular position of both joints will change in time in order to produce rhythmic patterns. The parameter sets in the cases of uncoupled, unidirectional and bidirectional two CPGs are $\{\alpha_1, \tau_1, E_1, \alpha_2, \tau_2, E_2\}$, $\{\alpha_1, \tau_1, E_1, a_{12}, b_{12}, \alpha_2, \tau_2, E_2\}$ and $\{\alpha_1, \tau_1, E_1, a_{12}, b_{12}, \alpha_2, \tau_2, E_2, a_{21}, b_{21}\}$, respectively. The Genetic Algorithm (GA) will be used to find the values of the parameters that optimize the objective function given below. The different walking patterns rely on this cost function:

$$J = -C_1 \sum_{k=1}^{n} x_b(k) + C_2 \left(\sum_{k=1}^{n} \left(\theta_1^2(k) + \theta_2^2(k) \right) \right) / n \quad (7)$$

where $C_1, C_2 \in [0,1]$ and $C_1 + C_2 = 1$, n is the number of elements of the position vector that is simulated with the objective of establishing patterns in order to maximize the displacement or velocity. When $C_2 = 0$, the energy consumption is ignored; hence, the displacement is maximized. Otherwise, when $C_1 = 0$, the energy consumption is minimized ignoring the displacement. It is obvious that for $C_1 = 0$, the minimum displacement is obtained when there is no locomotion. Therefore, throughout this study, it is assumed that $C_1 \neq 0$. Moreover, the requirement $C_1 + C_2 = 1$ is used just to balance the energy consumption and the total displacement.

The values of C_1 and C_2 are varied to clarify the relationship between the velocity and the energy constraints during CPG optimization. The second term in (6) is used to provide patterns, including smaller angular displacements for the legs. Consequently, this reduces the energy consumption. The ultimate goal here is to minimize the energy while altering the position (for more details on biological locomotion (Alexander, 1996; Nolfi and Floreano, 2000).

The two constraints revealed here are $0 \leq \theta_1,\ \theta_2 \leq \pi$ due to physical reasons. In the present study, a hybrid function is used during the optimization process which runs after the GA terminates for improving the value of the fitness function. The final point from GA is used as the initial point in either Pattern Search (PS) or fminsearch (FM) in MatLab.

It is observed that in both cases of the uncoupled and unidirectional two CPGs, either the leg does not move or it takes only a few steps in an unusual manner. However, locomotion can be achieved with the bidirectional two CPGs, as shown in Figs 20, 21, 22, 23 and 24 for both cases $C_1, C_2 \neq 0$ and $C_2 = 0$.

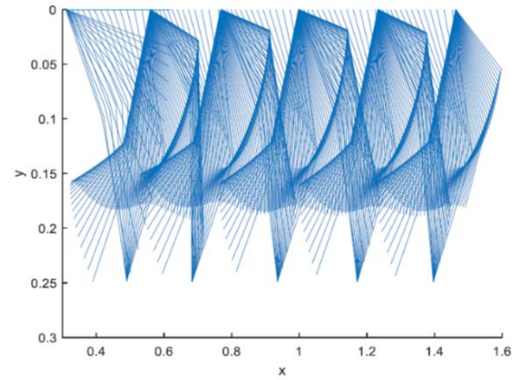

Fig. 20. One leg animation for bidirectional two CPGs: This animation corresponds to the values $\alpha_1 = 1.0695$, $\tau_1 = 1.2666$, $E_1 = 2.1157$, $a_{12} = 1.3610$, $b_{12} = 0.7478$, $\alpha_2 = 2.2222$, $\tau_2 = 1.9279$, $E_2 = 3.4393$, $a_{21} = 3.2908$, $b_{21} = 3.2794$ when $C_1, C_2 \neq 0$.

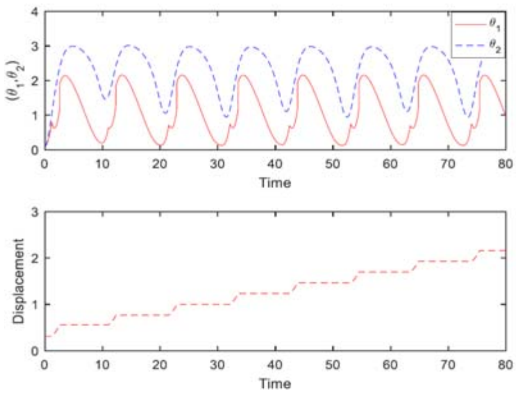

Fig. 21. Angles and displacement against time for bidirectional two CPGs when $C_1, C_2 \neq 0$: This solution corresponds to the same values in Fig 22.

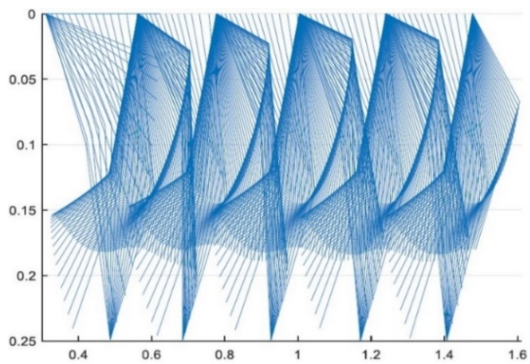

Fig. 22. One leg animation for bidirectional two CPGs: this animation corresponds to the values $\alpha_1 = 0.9855$, $\tau_1 = 1.2981$, $E_1 = 2.0748$, $a_{12} = 1.3475$, $b_{12} = 0.7401$, $\alpha_2 = 2.1861$, $\tau_2 = 1.9234$, $E_2 = 3.3872$, $a_{21} = 3.3011$, $b_{21} = 3.2758$ when $C_2 = 0$.

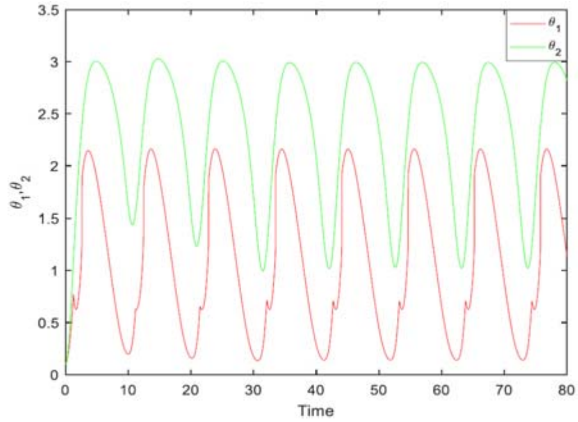

Fig. 23. Outputs of bidirectional two CPGs when $C_2 = 0$: This solution corresponds to the same values in Fig 24.

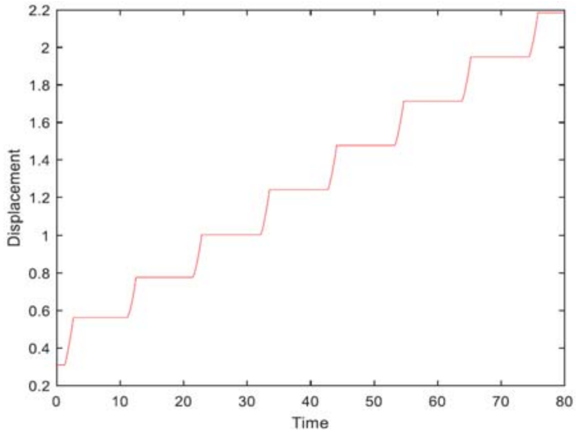

Fig. 24. Displacement against time for bidirectional two CPGs when $C_2 = 0$: This solution corresponds to the same values in Fig 24.

In fact, these optimization results supply the conclusion given in the stability analysis. Tables 1-6 summarize the results of this optimization for the three cases under investigation: uncoupled, unidirectional and bidirectional two CPGs, respectively. In all cases, J, x_b and E denote the values of the cost function, total displacement and energy, respectively.

Table 1. Optimization of uncoupled two CPGs when $C_1, C_2 \neq 0$.

Solver	Parameter values	J	x_b
GA	28.9834 36.2518 4.5906 111.2763 35.3121 9.8696	−2048.5	0.5271
GA	31.5979 36.3647 4.5536 110.8210 35.3333 9.8660	−2050.4	0.5299
GA with PS	32.9827 36.6254 4.5648 110.8486 35.2849 9.8694	−2052.7	0.5257
GA with FM	52.6429 61.4651 8.2096 18.6831 28.2615 6.9612	−1998	0.6037

Table 2. Optimization of uncoupled two CPGs when $\boldsymbol{C_2 = 0}$.

Solver	Parameter values	J	x_b
GA	43.4261 79.7966 14.7043 96.3819 41.6429 9.8691	−3916.3	0.5942
GA	44.4261 78.7966 14.2043 98.0069 41.7679 9.8691	−3915.6	0.5940
GA with PS	46.6724 79.0434 14.4197 100.0917 41.0695 9.8547	−3934	0.5951
GA with FM	54.3031 83.7118 11.7086 16.1890 33.7975 7.5507	−3870	0.6038

According to Tables 1 and 2, increasing optimization time or extending the region renders the leg unable to walk. Similarly, Tables 3 and 4 support the results given previously such that the leg is unable to walk normally.

Table 3. Optimization of unidirectional two CPGs when $\boldsymbol{C_1, C_2 \neq 0}$.

Solver	Parameter values	J	x_b
GA	23.8309 37.8704 2.2214 39.5901 20.4244 26.1536 33.2256 9.8616	−2367.3	0.6130
GA	57.1658 38.1815 2.1811 4.8573 24.7362 58.3004 47.0796 9.8694	−2257.4	0.6150
GA with PS	57.7655 38.1815 2.1811 4.8534 24.9237 58.3017 47.0796 9.8694	−2257.6	0.6151
GA with FM	59.5006 34.2580 2.2877 7.7744 30.2325 60.7280 39.4452 9.8668	−2336.9	0.6141

Table 4. Optimization of unidirectional two CPGs when $C_2 = 0$.

Solver	Parameter values	J	x_b
GA	19.1593 37.3610 2.4442 29.2822 23.7775 39.8811 31.5082 9.8595	−4798.6	0.6103
GA	16.6046 12.9354 0.2630 29.7203 25.9645 41.3522 38.5263 9.8690	−4722	0.6202
GA with PS	17.4443 12.7218 0.2635 32.9492 26.5549 59.7024 38.5626 9.8659	−4741	0.6194
GA with FM	16.8698 14.1344 0.2599 30.8606 26.4618 43.3883 42.3464 9.8660	−5259.9	0.6201

Table 5. Optimization of bidirectional Two CPGs when $\boldsymbol{C_1, C_2 \neq 0}$.

Solver	Parameter values	J	x_b	μ	β_1	β_2
GA	0.9999 1.9982 0.5233 2.4831 1.6538 0.8678 2.2644 2.6215 2.4274 1.6276	−877.5649	0.6204	0.4466	5.3960	0.4781
GA	1.0158 2.0092 0.5724 2.5768 1.6678 0.8976 2.2644 3.1261 2.4401 1.6481	−1810.7	0.6209	0.4372	5.3595	0.3586
GA with PS	1.0517 1.2945 2.0737 1.3461 0.7428 2.1834 1.9535 3.3817 3.2864 3.2522	−5078.9	2.1939	0.5460	−0.1025	2.4519
GA with FM	1.0520 1.2952 2.0771 1.3466 0.7448 2.1885 1.9547 3.3832 3.2922 3.2542	−5068.4	2.1966	0.5467	−0.1031	2.4671

Table 6. Optimization of bidirectional Two CPGs when $\boldsymbol{C_2 = 0}$.

Solver	Parameter values	J	x_b	μ	β_1	β_2
GA	0.9961 1.0081 0.5403 2.3114 0.4843 0.9942 1.9538 2.3390 2.9803 2.6291	−2411.2	0.6211	0.1848	8.7829	1.4235
GA	1.0033 1.0088 0.5403 2.3375 0.4844 0.9942 1.9539 2.3381 2.9809 2.6721	−4904.6	0.6222	0.1858	9.0636	1.4250
GA with PS	0.9855 1.2981 2.0748 1.3475 0.7401 2.1861 1.9233 3.3868 3.3011 3.2758	−10286	2.1852	0.5451	−0.0948	2.5206
GA with FM	0.9940 1.3046 2.1067 1.3529 0.7216 2.2720 1.9025 3.4102 3.3188 3.3236	−10332	2.2126	0.5342	−0.0999	2.6629

In Tables 5 and 6, in contrast, the leg is able to move. When the fixed points are unstable, optimizing the bidirectional two CPGs cannot produce rhythmic patterns.

Experiments relying on the value of μ, β_1 and β_2 show that when the fixed points are stable, the velocity and displacement increase by increasing the values of τ and α. Moreover, when the angles are kept in the region $[0, 6\pi/7]$, to be more consistent with real life, the locomotion becomes better than the angles kept between $[0, \pi]$, as shown in Figs 25 and 26. The parameters of the coupling weights are important in order to balance the disturbance during optimization. Moreover, when the parameters α and $\tau \in (0,3]$, the bidirectional two CPGs are definitely able to generate different RPs for one leg to move; these RPs generate different types of locomotion when the couple parameters a_{ij} and $b_{ij} \in [-2,3]$. It is certain that it is possible to generate the rhythmic patterns by optimizing the bidirectional two CPGs outside of the above regions.

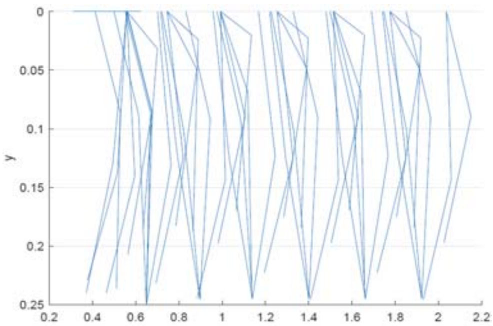

Fig. 25. One leg animation in the case of Bidirectional two CPGs in 4 sec: This animation corresponds to the values $\alpha = 0.9480$, $\tau = 0.1011$, $E_1 = 2.6940$, $a_{12} = 1.3219$, $b_{12} = 0.1477$, $E_2 = 2.0899$, $a_{21} = 2.4394$, $b_{21} = -0.00005$.

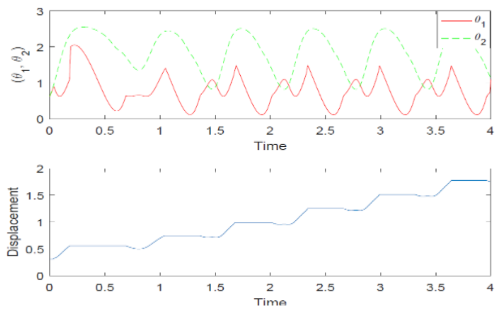

Fig. 26. Outputs of CPGs and displacement against time for Bidirectional two CPGs in 4 secs: This solution corresponds to the same values in Fig 25.

6. CONCLUSIONS

This paper focuses on three cases of CPGs: uncoupled, unidirectional and bidirectional two CPGs. These couplings are used to produce rhythmic patterns for one leg with two degrees of freedom. When the optimization is performed in the first two cases, CPGs are unable to provide the basic locomotor rhythm patterns for the leg. In contrast, by utilizing the bidirectional two CPGs, the results show far greater improvement than in the other cases. The bidirectional coupling yields the best performance level. Results also reveal that when τ and α are close to zero and the fixed points are stable, the velocity and displacement increase. That is, changes in the CPG parameters may produce different results. Of course, not only the values of τ and α are important, but also in the bidirectional two CPGs, the couple weight a_{ij} and b_{ij} that drive the system to two diverging phases, which lead to obtain the conflicting perturbations, these perturbations are influenced by the energies E_{j} of bidirectional two CPGs. For instance, during the experiment, when the amplitude of the second CPG is very small, the coupling weight will be definitely week, in order to reach the strength of coupling CPGs to be independent from the amplitude of the emitting CPG, then, the bidirectional two CPGs are able to generate rhythmic patterns for the leg to move along x-direction in the stable region. The rhythmic motions rely on coupling weights a_{ij} and b_{ij} and the values of both parameters τ and α. This study indicates that not only do CPGs in the spinal cord of humans influence human locomotion, they also take over the locomotion without any provided sensory feedback. To the extent that bidirectional two CPGs are the most effective essentials akin to real life-induced rhythmic patterns, it is reasonable for them to be considered pivotal features most conducive to locomotion. The results of the study warrant broader future applications of bidirectional two CPGs of the third type to account for a variety of upper limb locomotion. These results are important, then not only because of what they may contribute to the ongoing discussion of locomotion but also for the support that they give to bidirectional two CPGs as a critical aspect of locomotion. These results pave the way for further research into CPGs as potential controllers of upper limbs for different movements.

ACKNOWLEDGEMENT

The authors acknowledge the support of the Lab Technicians at Atılım University for their assistance in addition to the valuable suggestions made by Prof.Dr. Senih Gürses from the Middle East Technical University

REFERENCES

Alexander, R. M. (1996). Optima for animals: Princeton University Press.

Amrollah, E., & Henaff, P. (2010). On the role of sensory feedbacks in Rowat–Selverston CPG to improve robot legged locomotion. Frontiers in neurorobotics, 4, 113.

Aoi, S., & Tsuchiya, K. (2005). Locomotion control of a biped robot using nonlinear oscillators. Autonomous robots, 19(3), 219-232.

Arena, P. (2000). The central pattern generator: A paradigm for artificial locomotion. Soft Computing, 4(4), 251-266.

Arena, P. (2001). A mechatronic lamprey controlled by analog circuits. Paper presented at the Proceedings of the 9th IEEE mediterannean conference on control and automation.

Arena, P., Fortuna, L., Frasca, M., & Sicurella, G. (2004). An adaptive, self-organizing dynamical system for hierarchical control of bio-inspired locomotion. IEEE Transactions on Systems, Man, and Cybernetics, Part B (Cybernetics), 34(4), 1823-1837.

Arikan, K. B., & Irfanoglu, B. (2011). A Test Bench to Study Bioinspired Control for Robot Walking. Journal of Control Engineering and Applied Informatics, 13(2), 76-80.

Billard, A., & Ijspeert, A. J. (2000). Biologically inspired neural controllers for motor control in a quadruped robot. Paper presented at the Neural Networks, 2000. IJCNN 2000, Proceedings of the IEEE-INNS-ENNS International Joint Conference on.

Brambilla, G., Buchli, J., & Ijspeert, A. J. (2006). Adaptive four legged locomotion control based on nonlinear dynamical systems. Paper presented at the International Conference on Simulation of Adaptive Behavior.

Bucher, D., Haspel, G., Golowasch, J., & Nadim, F. (2000). Central pattern generators. eLS.

Casasnovas, B., & Meyrand, P. (1995). Functional differentiation of adult neural circuits from a single embryonic network. The Journal of neuroscience, 15(8), 5703-5718.

Crespi, A., & Ijspeert, A. J. (2006). AmphiBot II: An amphibious snake robot that crawls and swims using a central pattern generator. Paper presented at the Proceedings of the 9th international conference on climbing and walking robots (CLAWAR 2006).

Crespi, A., & Ijspeert, A. J. (2008). Online optimization of swimming and crawling in an amphibious snake robot. IEEE Transactions on Robotics, 24(1), 75-87.

Elbori et al (2017). Optimization of Central Patterns Generators. Journal of engineering and applied sciences 12(5), 1164-1172.

Endo, G., Nakanishi, J., Morimoto, J., & Cheng, G. (2005). Experimental studies of a neural oscillator for biped locomotion with QRIO. Paper presented at the Proceedings of the 2005 IEEE international conference on robotics and automation.

Fukuoka, Y., Kimura, H., & Cohen, A. H. (2003). Adaptive dynamic walking of a quadruped robot on irregular terrain based on biological concepts. The International Journal of Robotics Research, 22(3-4), 187-202.

Ijspeert, A. J. (2008). Central pattern generators for locomotion control in animals and robots: a review. Neural Networks, 21(4), 642-653.

Ijspeert, A. J., & Cabelguen, J.-M. (2006). Gait transition from swimming to walking: investigation of salamander locomotion control using nonlinear oscillators Adaptive Motion of Animals and Machines (pp. 177-188): Springer.

Ijspeert, A. J., & Crespi, A. (2007). Online trajectory generation in an amphibious snake robot using a lamprey-like central pattern generator model. Paper presented at the Proceedings 2007 IEEE International Conference on Robotics and Automation.

Ijspeert, A. J., Crespi, A., Ryczko, D., & Cabelguen, J.-M. (2007). From swimming to walking with a salamander robot driven by a spinal cord model. science, 315(5817), 1416-1420.

Inada, H., & Ishii, K. (2003). Behavior generation of bipedal robot using central pattern generator (CPG)(1st report: CPG parameters searching method by genetic algorithm). Paper presented at the Intelligent Robots and Systems, 2003.(IROS 2003). Proceedings. 2003 IEEE/RSJ International Conference on.

Inagaki, S., Yuasa, H., & Arai, T. (2003). CPG model for autonomous decentralized multi-legged robot system—generation and transition of oscillation patterns and dynamics of oscillators. Robotics and Autonomous Systems, 44(3), 171-179.

Inagaki, S., Yuasa, H., Suzuki, T., & Arai, T. (2006). Wave CPG model for autonomous decentralized multi-legged robot: Gait generation and walking speed control. Robotics and Autonomous Systems, 54(2), 118-126.

Ishiguro, H., Ono, T., Imai, M., & Kanda, T. (2003). Development of an interactive humanoid robot “Robovie”—an interdisciplinary approach Robotics Research (pp. 179-191): Springer.

Jiaqi, Z., Masayoshi, T. Z., Qijun, C., & Chengju, L. (2011). Dynamic walking of AIBO with Hopf oscillators. Chinese Journal of Mechanical Engineering, 24(4), 612-617.

Kimura, H., Akiyama, S., & Sakurama, K. (1999). Realization of dynamic walking and running of the quadruped using neural oscillator. Autonomous robots, 7(3), 247-258.

Kimura, H., Fukuoka, Y., & Cohen, A. H. (2007). Adaptive dynamic walking of a quadruped robot on natural ground based on biological concepts. The International Journal of Robotics Research, 26(5), 475-490.

Lu, Z., Ma, S., Li, B., & Wang, Y. (2005). Serpentine locomotion of a snake-like robot controlled by cyclic inhibitory CPG model. Paper presented at the 2005 IEEE/RSJ International Conference on Intelligent Robots and Systems.

Marbach, D. (2004). Evolution and Online Optimization of Central Pattern Generators for Modular Robot Locomotion. Unpublished Master Thesis, Swiss Federal Institute of Technology Lausanne.

Nachstedt, T., Tetzlaff, C., & Manoonpong, P. (2017). Fast Dynamical Coupling Enhances Frequency Adaptation of Oscillators for Robotic Locomotion Control. *Frontiers in neurorobotics, 11*.

Nolfi, S., & Floreano, D. (2000). *Evolutionary robotics: The biology, intelligence, and technology of self-organizing machines*: MIT press.

Pinto, C. M., & Golubitsky, M. (2006). Central pattern generators for bipedal locomotion. *Journal of mathematical biology, 53*(3), 474-489.

Sillar, K. T. (1996). The development of central pattern generators for vertebrate locomotion. *Advances in Psychology, 115*, 205-221.

Taga, G. (1998). A model of the neuro-musculo-skeletal system for anticipatory adjustment of human locomotion during obstacle avoidance. *Biological cybernetics, 78*(1), 9-17.

Taga, G., Yamaguchi, Y., & Shimizu, H. (1991). Self-organized control of bipedal locomotion by neural oscillators in unpredictable environment. *Biological cybernetics, 65*(3), 147-159.

Torres-Huitzil, C., & Girau, B. (2008). *Implementation of central pattern generator in an FPGA-based embedded system.* Paper presented at the International Conference on Artificial Neural Networks.

Van den Kieboom, J. (2009). Biped locomotion and stability: a practical approach.

Van Vreeswijk, C., Abbott, L., & Ermentrout, G. B. (1994). When inhibition not excitation synchronizes neural firing. *Journal of computational neuroscience, 1*(4), 313-321.

Wang, T., Chevallereau, C., & Tlalolini, D. (2014). Stable walking control of a 3D biped robot with foot rotation. *Robotica, 32*(4), 551-570.

Williamson, M. M. (1999). *Robot arm control exploiting natural dynamics.* Massachusetts Institute of Technology.

Wu, X., Teng, L., Chen, W., Ren, G., Jin, Y., & Li, H. (2013). CPGs With Continuous Adjustment of Phase Difference for Locomotion Control. *International Journal of Advanced Robotic Systems, 10*.